

Guarded Hot-Plate (GHP) Method: Uncertainty Assessment

U. Hammerschmidt¹

Received November 13, 2001

In civil engineering, the thermal conductivity is the most important quantity for thermal insulations and, as such, is in most cases determined with the guarded hot plate instrument in accordance with the applicable standards. These standards are to assure that uniform and reliable measurements will lead to comparable results. In addition, the quality of a measurement result essentially depends on its measurement uncertainty which, for reasons of acceptance, should also be determined according to a uniform guideline. For some time now, such a standard has been available: The ISO “*Guide to the Expression of Uncertainty in Measurement*,” often abbreviated to GUM. Its application will be demonstrated comprehensively, and in detail, by the example of a guarded hot plate instrument which can be used at working temperatures from -70 to 200°C . The terms and definitions of the GUM required for this purpose will be extended by the instrument-and-sample-specific corrections and used as a basis for establishing the uncertainty budget. As far as possible, both alternatives offered by the GUM—type A and type B methods—are used in parallel. The combination of the sensitivity coefficients and variances of the budget yields the expanded standard uncertainty of the specific guarded hot plate instrument examined. In this case, it is 1.9% at 20°C .

KEY WORDS: guarded hot plate; ISO GUM; standard uncertainty; thermal conductivity.

1. INTRODUCTION

Although the usage of transient techniques has increased substantially in the past twenty years, in Europe, guarded hot plate (GHP) instruments are still the work horses for measuring the thermal conductivity λ of insulating materials. The conductivity range covered has its upper limit at about

¹Physikalisch-Technische Bundesanstalt, Bundesallee 100, 38116 Braunschweig, Germany.
E-mail: ulf.hammerschmidt@ptb.de

$6 \text{ W} \cdot \text{m}^{-1} \cdot \text{K}^{-1}$ and its lower one at some $0.01 \text{ W} \cdot \text{m}^{-1} \cdot \text{K}^{-1}$. Working temperatures can approach the boiling point of nitrogen ($\sim 78 \text{ K}$) on one extreme end of the scale and the melting point of iron ($\sim 1810 \text{ K}$) on the other [1].

Since only measurements of the base quantities length, temperature, and electrical power are required, a GHP instrument is an absolute or fundamental one. Therefore, it can be used for traceability reasons and certification of reference materials of low conductivity. Commercially, thermal insulations, some masonry products, and low density insulating refractories are mostly analyzed.

Though the design of a GHP apparatus is a complex subject and operating it requires great care and time, its reliability is remarkably high and its uncertainty can be comparatively low. As the major indication of the quality of a measurement result, the uncertainty should be identified following an internationally accepted procedure.

In 1992, a common basis for international comparisons of measurement results was constituted by ISO, the International Organization for Standardization, and other organizations. Their *Guide to the Expression of Uncertainty in Measurement* (GUM) [6] provides general rules for the assessment of uncertainties as well as for the values of appropriate influence quantities.

In close accordance to the GUM, the uncertainty of the guarded hot plate instrument, "GHP-S," of the Physikalisch-Technische Bundesanstalt (PTB) was determined. For this purpose, the two different procedures of the GUM, i.e., type-A and type-B evaluations, are used in parallel as far as possible.

This report begins with a short description of terms and definitions concerned with the ISO standard uncertainty. Next, the instrument mentioned is presented briefly. In the fourth section its underlying ideal mathematical model is defined. Due to unavoidable imperfections, instrument errors occur. These are identified subsequently within the framework of a real model that, as far as possible, is compensated by correction factors for the instrument and sample geometry.

2. TERMS AND DEFINITIONS

It is the objective of a measurement to determine the value of a physical quantity. However, in this determination unavoidable influence quantities occur so that the measured values scatter around the value of the quantity searched. Therefore, the result of a measurement, y , is only an estimate of the measurand Y . The quality of the estimator can be characterized by the dispersion of the values and is processed according to a suitable statistical

procedure and stated in the measurement result as its uncertainty $u(y)$. From among the different possible measures of scatter, the ISO GUM selects the square root from the variance $u^2(y)$ of the measurement value and denotes the parameter in the GUM as “standard uncertainty.” For the “combined standard uncertainty,” Eq. (1), the choice of the square deviation as the measure of evaluation leads to outliers being relatively more strongly evaluated within the scope of the uncertainty budget (cf., Section 5.4) than in the case of linear addition.

Only seldom can the output quantity y be measured directly. In most cases it must be determined indirectly on the basis of a functional relationship $y = f(\vec{x})$ from other measurands, the input quantities x_i . The respective scatter of these, leads to individual variances $u^2(x_i)$ of all N input quantities (partial measurements). They are combined with the aid of the Gaussian law of propagation of uncertainty to form the “combined variance” $u_c^2(y)$ of the output quantity:

$$u_c^2(y) = \sum_{i=1}^N \left(\frac{\partial f(x)}{\partial x_i} \right)^2 u^2(x_i). \quad (1)$$

In Eq. (1) the influence of every input quantity x_i on the “combined standard uncertainty” $u_c(y)$ by the associated “sensitivity coefficient” $\partial f(x)/\partial x_i$ is taken into account.

For the determination of the variances of the input quantities, $u^2(x_i)$, the GUM offers two alternative methods: the type A and the type B methods. The type A method is a purely statistical analysis of series of observations as it is also represented in the relevant textbooks (e.g., Ref. 14). It describes the determination of the (empirical) variance of the quantity x_i from N observations. From a series of observations $[x_{ij}]$ first the mean value \bar{x}_{i0} is calculated according to the relation

$$\bar{x}_{i0} = \frac{1}{N} \sum_{j=1}^N x_{ij} \quad (2)$$

and then the (empirical) variance from

$$u^2(x_i) = \frac{1}{N-1} \sum_{j=1}^N (x_{ij} - \bar{x}_{i0})^2. \quad (3)$$

The variance according to Eq. (3) is referred to as an empirical variance, since it is based only on a limited, finite number N of observations. To obtain fairly reliable values for the variance, the number of observations should be greater than 10.

The best estimate to be associated with x_i is given by the variance of the mean

$$u^2(\bar{x}_{i0}) = \frac{1}{N} u^2(x_{i0}) \quad (4)$$

The standard uncertainty of x_i is the estimated standard deviation of the mean, $u(\bar{x}_{i0})$, the positive square root of $u^2(\bar{x}_{i0})$.

The alternative, type B, method is based on information “other than statistical.” This so-called “metrologically founded assessment” relies on relevant values from other measurements, from manufacturers, from calibration certificates or the like. Frequently, only the upper and lower limits, a_+ and a_- , can be stated for the value x_i of a quantity. Then, with

$$x_i = \frac{1}{2} (a_+ + a_-) \quad (5)$$

the following is valid as the variance:

$$u^2(x_i) = \frac{1}{12} (a_+ - a_-)^2 = \frac{1}{3} a^2 \quad (6)$$

where $2a = a_+ - a_-$.

To determine the uncertainty, a stepwise procedure is recommended as follows:

1. analysis of the measuring principle
2. formulation of the functional relation between output quantity (y) and input quantities (x_1, x_2, x_3, \dots): ideal model
3. significant corrections are identified and applied: experimental model
4. all sources of uncertainty are listed in an uncertainty analysis (budget)
5. determination of uncertainty and statement as “expanded uncertainty.”

3. EXPERIMENTAL SETUP

3.1. Apparatus

The single plate GHP apparatus “GHP-S” of PTB measures the thermal conductivity $\lambda(T)$ of solids between 0.01 and $6 \text{ W} \cdot \text{m}^{-1} \cdot \text{K}^{-1}$ as a function of temperature T between -80 and 200°C (cf., e.g., Ref. 7).

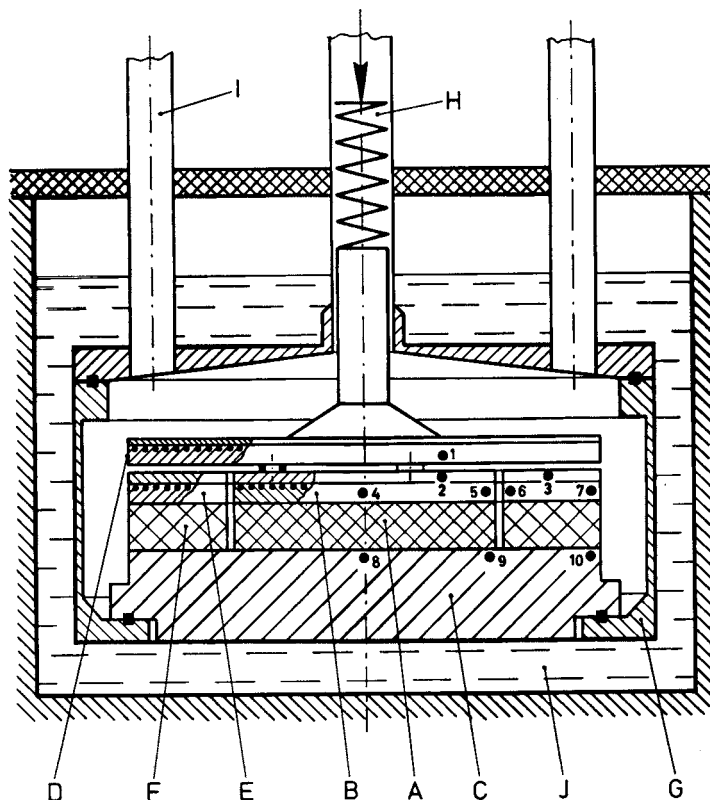


Fig. 1. Schematic of the Guarded Hot Plate Apparatus "GHP-S." A, specimen; B, hot plate; C, cold plate; D, guard plate; E, guard ring; F, edge insulation; G, casing; H, push rod; I, ducts; J, thermostated bath; 1-10, thermocouples.

The guarded hot plate (Fig. 1) is designed as a stack and accommodated in the evacuable casing (G). The cylindrical solid sample (A) with the cross-sectional area A and the thickness d is placed between the upper electrical hot plate (B) and the lower thermostated cold plate (C). On its lateral face the sample is surrounded by edge insulation (F). The hot plate dissipates the constant electric input power $P = UI$ as the heat flow-rate P , which on its way to the cold plate traverses the sample as homogeneously as possible. The known heat flow leads to a temperature drop ΔT across the sample which is the measure of its thermal conductivity. Two guard heaters, the guard plate (D) and the guard ring (E) that surround the hot plate are intended to establish a unidirectional and uniform heat flow of rate P . A push rod (H) which can be adjusted from outside ensures that the

stack remains tightly packed without the sample being compressed. The working temperature T_A is set by immersion of the whole apparatus in a bath thermostat (J). All temperature measuring points of the apparatus are identified by the numbered points in Fig. 1.

The peripheral equipment consists of three constant-current sources to supply the two active guard heaters and the hot plate, a standard measuring resistor to accurately determine the current supplied to the hot plate, a twelve-channel measuring point selector switch (scanner), and a digital nanovoltmeter (DVM). The instrumentation is connected to a PC by a general-purpose bus (IEEE-488). The PC uses a PID control program to bring the guarded hot plate into steady state ($\Delta T = \text{const.}$) and, subsequently collects the relevant measurement data for evaluation. During every measurement cycle, every electric input quantity (cf., Eq. (7), Section 4.1) such as voltage and current of the hot plate as well as the thermoelectric voltages of the copper-constantan thermocouples, is scanned in twelve individual measurements and processed after the mean value has been calculated. All peripheral devices, as well as the thermocouples, are calibrated and subjected to internal quality control at regular intervals.

3.2. Specimen

The ideal specimen is shaped like a right circular cylinder of length d ($5 \text{ mm} \leq d \leq 25 \text{ mm}$) and 100 mm in diameter. In practice, the specimen should approach a cylinder as close as possible: the diameter at the ends of the specimen is constrained to $100 \text{ mm} \pm 0.01 \text{ mm}$ or better to match the hot and cold plates of the measuring instrument. The deviations from plane parallelism should not exceed $\pm 0.01 \text{ mm}$. The bases are precisely levelled to $\pm 0.02 \text{ mm}$; if possible, they are highly polished. Before measurements are initiated, the specimen is carefully checked that it has been prepared in accordance with the appropriate material specifications and conditioned if necessary.

To promote good thermal contact between the specimen and the hot and cold plates, rigid (nonporous) specimen materials are coupled to both plates by the use of a contact medium. Generally, silicone oil "DC 200" ($\nu(20^\circ\text{C}) = 12500 \text{ mm}^2 \cdot \text{s}^{-1}$) is used. At temperatures $T \leq -45^\circ\text{C}$, helium is employed. In the latter case, there are three aluminium spacers mounted between the sample and each plate to set up a gas layer of known thickness.

To connect porous materials (e.g., bricks) to both plates, silicone oil can be used as well. However, prior to the assembly of the specimen in the apparatus, the specimen is sealed with a very thin protective film that is sprayed on.

Loose fill materials can be placed in a shallow box of thin-walled low conductivity material having outside dimensions as given above. The box is then coupled to both plates by the use of oil.

4. THEORY

4.1. Ideal Model

For the development of the theory presented below, it is useful to start with an ideal model, i.e., a model for a perfect GHP instrument that yields the correct value of the quantity measured. For the ideal single-plate GHP and a homogeneous and isotropic sample with conductivity λ that is assumed to be opaque to radiation, e.g., DIN 52612 [2] specifies the following equation:

$$\lambda = \frac{P \cdot d}{A(T_2 - T_1)}. \quad (7)$$

Here, T_1 and T_2 denote the temperatures of the cold and hot sides of the sample, respectively. The measured value for the thermal conductivity, $\lambda_m = \lambda(T_m)$, is to be related to the mean temperature $T_m = (T_1 + T_2)/2$.

However, the above model is inadequate for practical purposes. Unavoidable experimental influence quantities lead to deviations from perfect behavior resulting in a difference between the correct value and the experimental estimate. Therefore, the model presented must be modified to a real model.

The difference between the correct value and the estimate is known as the experimental error. There are two major sources of experimental error, systematic and random effects. Random effects exhibit a statistical distribution and thus, random errors cannot be anticipated. They are equal to error minus systematic error. A systematic error is repeatable.

Systematic errors can be subdivided into intrinsic and external errors. Any inconstancy of the working temperature T_A , for example, exerts a substantial external influence. The sources of the intrinsic errors are to be found in the design of the apparatus (stray heat flows, thermal contact resistances,...) and the properties of the real sample specifically prepared for the apparatus (deviations from the prescribed geometry, inhomogeneities,...).

As a result of the repeatability of systematic errors, quantifiable components of them should be compensated by corrections. The ideal model therefore must be extended by the significant corrections to obtain the mathematical model for the experiment.

Blunders (careless errors), errors resulting from procedural or computational errors, are not discussed in the framework of this report.

4.2. Real Model

4.2.1. Systematic Measurement Errors

According to the ideal mathematical model [Eq. (7)], the thermal conductivity, $\lambda = f(x_1, x_2, x_3, x_4, x_5)$, is determined from the results of five partial measurements: (1) the heat flow $P = x_1$, (2) and (3) the two temperatures $T_1 = x_2$ and $T_2 = x_3$, as well as (4) the thickness of the sample, $d = x_4$, and (5) its cross-sectional area, $A = x_5$.

According to their source, the intrinsic systematic errors are subdivided into two classes: apparatus- and specimen-specific deviations, as listed in Table I. Among the apparatus-specific errors given in that table, the first four deviations influence the rate of heat flow P as stray heat flows P_{Vi} . The errors of the temperature measurement with the thermocouples used for this purpose are determined by a procedure which is described in detail in Ref. 8 and also assigns them to the measurand P . The errors due to the thermal expansion of the apparatus plates and the thermal expansion of the sample are analyzed together. The errors due to the indirect measurement of the temperatures T_1 and T_2 in bore holes of the hot and cold plates (instead of the hot and cold sample surfaces) are assigned to the quantities T_1 and T_2 . The sample-specific errors mentioned—except for thermal expansion—must be separately determined from specimen to specimen.

4.2.1.1. Apparatus-Specific Errors

The total heat flow P that is supplied as the electric power output of the hot plate, consists of seven components, viz., the net heat flow P_0 traversing the sample and the six different stray heat flows P_x and P_{Vi} :

$$P = P_0 + P_x - \sum_{i=1}^5 P_{Vi} \quad (8)$$

Table I. Significant Systematic Errors

Measurand	Apparatus	Measurand	Specimen
P_{V1}, P_{V2}	Unbalance error	P_A	Thermal resistance
P_{V3}, P_{V4}	Edge heat loss error (gap)	P_S	Radiative heat transfer
P_{V5}	Edge heat loss error (sample)	ΔT_S	Temperature jump
P_x	Thermocouples		
d, A	Therm. expansion of plates	d, A	Therm. expansion of sample
$\Delta T_b, \Delta T_c$	Indirect temperature measurement		

The five stray heat flows P_{Vi} are discussed first:

(a) Imbalance error, ($i = 1, 2$)

Source: Due to temperature differences between the hot plate and the guard plate (component $i = 1$) or the guard ring ($i = 2$), respectively, there are stray heat flows between these related parts of the instrument.

Determination: (Woodside and Wilson procedure [9, 10]).

By thermal mismatching of the instrument parts in question with respect to one another, a material-specific straight line $\lambda = f(\Delta T)$ can be obtained:

$$P_{Vi} = C_i \Delta T_i, \quad (i = 1, 2) \quad (9)$$

$$P_{V1} = C_1 \Delta T_1 = C_1(T_2 - T_1) \quad (10)$$

$$P_{V2} = C_2 \Delta T_2 = C_2 \left[\frac{(T_2 + T_5)}{2} - \frac{(T_3 + T_6)}{2} \right] \quad (11)$$

(b) Edge Heat Loss Error (hot plate), ($i = 3, 4$)

Source: As there are no heaters in the two air-filled gaps between the hot plate and the guard ring ($i = 3$) or the guard plate ($i = 4$), respectively, the hot plate suffers the heat loss P_{Vi} .

Determination: (Fritz and Bode procedure (cf., Refs. 11 and 12, also DIN 52612)).

The heat loss P_V is determined from the surface area of the gap (A_{Sp}) and the thermal conductivity of the material below the gap (λ_{Sp}) as well as from the temperature difference ΔT :

$$P_{Vi} = \left(\frac{\lambda_{Sp} A_{Sp}}{2} \right) \frac{\Delta T_i}{d} \quad (i = 3, 4) \quad (12)$$

(c) Edge Heat Loss Error (sample), ($i = 5$)

Source: As a result of a temperature difference between the edge of the sample (lateral surface) and the environment, a stray heat flow may be produced.

Determination: Analytical procedure according to Bode [12], various finite-element procedures (e.g., Ref. 13).

(d) Thermocouple, (P_X)

The measurement errors of the thermocouples are due to small individual differences of the thermoelectric power with the temperature differences being identical. The correction factor P_X is determined in two series of measurements (marked * and **) according to a procedure described in detail in Ref. 8.

Table II. Properties and Sequence of Layers Between Temperature Stations (T_4 & T_8 and T_5 & T_9) and Sample Surface (cf. text)

Layer	Material	Thickness (mm)
1	Copper	3.3
2	Nickel	0.04
3	Contact medium (gas, oil,...)	15×10^{-6}

Heat flow from deviations in ΔT :

$$P_x = \frac{(P_z^* \Delta T^{**} - P_z^{**} \Delta T^*)}{(\Delta T^* - \Delta T^{**})} \quad (13)$$

Here, $P_z^* = P - \sum P_v$ denotes the correction factor "heat flow" from first series of measurements and $\Delta T^{**} = \Delta T$ is the correction factor "temperature difference" from second series of measurements.

(e) Indirect temperature measurement

The temperature difference ΔT across the sample is indirectly determined in two pairs of measurement points (T_4 and T_8 , and T_5 and T_9). The copper-constantan thermocouples ($\varnothing = 0.2$ mm) are located in bore holes in the nickel-plated copper plates. Their spacing from the respective sample surface is composed of the layer thicknesses according to Table II.

For the Pyrex specimen, silicone oil is used as a contact medium. The thermal conductivities λ_i of copper, nickel, helium and silicone oil are known with an uncertainty $u(\lambda_i) \leq 2\%$ over the whole temperature range covered. With the further knowledge of the cross section area A of the specimen and the density of the oil, the mean thickness of the oil layer is determined by weighing.

Temperature drop across the sample:

$$\Delta T = \Delta T_0 - (\Delta T_b + \Delta T_c) \quad (14)$$

Temperature drop (measured):

$$\Delta T_0 = \frac{T_4 + T_5}{2} - \frac{T_8 + T_9}{2} \quad (15)$$

Temperature drop in the plate:

$$\Delta T_b = \frac{P \sum_{i=1}^2 (d_i / \lambda_i)}{A} \quad (16)$$

Temperature drop in the contact medium:

$$\Delta T_c = \frac{Pd_3}{A} \lambda^{-1} \quad (17)$$

4.2.1.2. Specimen-Specific Errors

(a) Thermal expansion of the sample

Source: At working temperatures T_A that differ from the room temperature T_0 , the volume of the sample changes as a result of thermal expansion. The variation of the specimen thickness and area affects the determination of the heat flow density.

Determination: The thickness variation is calculated with the known thermal expansion coefficient α of the specimen material:

Specimen thickness:

$$d = d_0[1 + \alpha(T_A - T_0)] \quad (18)$$

Specimen area:

$$A = \pi r^2 \quad r = r_0[1 + \alpha(T_A - T_0)] \quad (19)$$

(b) Contact Resistance Error

Source: The heat flowing from the hot plate to the cold plate traverses the two contact layers (coupling layers) S_1 and S_2 located above and below the sample. The layers have thicknesses d_1 and d_2 , and corresponding thermal conductivities λ_1 and λ_2 , which affect the heat flow as shown below.

Determination: The thermal contact is minimized with a suitable contact medium (oil, gas), if possible (cf., Section 3.2). The thermal conductivity λ_i and thickness d_i of the contact layer is known.

$$P_A = \frac{A}{\sum_{i=1}^3 (d_i/\lambda_i)} \Delta T \quad (20)$$

(c) Temperature jump

Source: Both on the upper and on the lower side of the sample, a temperature jump ΔT_i is produced, which depends on the heat flow density and the mechanical condition of the contact areas. The accommodation coefficient α' is a measure of the temperature jump.

Determination: Table values (as far as available).

(d) Exchange of radiation

Source: When the specimen is transparent to temperature radiation, the heat released from the hot plate is transmitted not only by conduction but also by radiation.

Determination: Experimental estimate of the radiative exchange by variation of the specimen thickness as well as of the temperature difference across the sample. As an alternative, a theoretical approximation can be calculated with the aid of infrared absorption spectra.

4.2.2. Model of the Guarded Hot Plate

In the real model of the single guarded hot plate, Eq. (21), all apparatus-specific corrections mentioned above have been taken into account. The following is obtained:

$$\begin{aligned}\lambda(T_m) &= \frac{P_0 - P_x - \sum_{i=1}^3 P_{vi}}{\pi[r_0(1 + \alpha(T_0 - T_m))]^2} \frac{d_0[1 + \alpha(T_0 - T_m)]}{\Delta T_0 - (\Delta T_b + \Delta T_c)} \\ \lambda(T_m) &= \frac{P_0 - P_x - \sum_{i=1}^3 P_{vi}}{\pi r_0^2 [1 + \alpha(T_0 - T_m)]} \frac{d_0}{\Delta T_0 - \Delta T_b - \Delta T_c} \\ &= \frac{Z_1}{N_1} \frac{Z_2}{N_2}\end{aligned}\quad (21)$$

In these relations, the thermal expansion coefficient α , its reference temperature T_0 ($=23^\circ\text{C}$), and the mean temperature T_m are considered to be constant.

4.2.3. Validity of the Model

The mathematical model, Eq. (21), valid for the following ranges of thermal and mechanical properties:

1. Range of measurement in $\text{W} \cdot \text{m}^{-1} \cdot \text{K}^{-1}$: $0.01 < \lambda < 6$
2. Mean temperature in $^\circ\text{C}$: $-75 < T < 195$
3. Heat flow in W : $0 < P_0 < 120$
4. Temperature difference in K : $5 < \Delta T < 20$
5. Sample thickness in mm : $5 < d < 25$
6. Temperature gradient in $\text{K} \cdot \text{m}^{-1}$: $\leq 3 \times 10^3$
7. Sample diameter in mm : 100
8. Sample area in mm^2 : 7853.98

The subsequent evaluation of the standard uncertainty is assessed with the following values as obtained from a measurement on the standard reference CRM 039 (Pyrex 7740) which has been taken as a concrete example. The Pyrex 7740 glass was manufactured by Corning France.

1. Thermal conductivity in $\text{W} \cdot \text{m}^{-1} \cdot \text{K}^{-1}$: 1.13
2. Working temperature in $^{\circ}\text{C}$: 20
3. Heat flow in W : 8.9
4. Temperature difference in K : 10
5. Sample thickness in mm : 10
6. Temperature gradient in $\text{K} \cdot \text{m}^{-1}$: 1000
7. Sample diameter in mm : 100
8. Sample area in mm^2 : 7853.98

5. STANDARD UNCERTAINTY

5.1. Variances

The combined standard uncertainty $u_c(y)$ is defined by Eq. (1). In the mathematical model, Eq. (21), all input quantities are assumed uncorrelated. Thus, the following equations are valid:

$$u_c^2(\lambda) = c_P^2 u^2(P) + c_A^2 u^2(A) + c_{\Delta T}^2 u^2(\Delta T) + c_d^2 u^2(d) \quad (22)$$

with:

$$c_P^2 u^2(P) = c_{P_0}^2 u^2(P_0) + c_{P_x}^2 u^2(P_x) + c_{\Sigma PV}^2 u^2(P_V) \quad (23)$$

$$c_A^2 u^2(A) = c_{r_0}^2 u^2(r_0) + c_{\alpha}^2 u^2(\alpha) + c_{T_0}^2 u^2(T_0) + c_{T_m}^2 u^2(T_m) \quad (24)$$

$$c_d^2 u^2(d) = c_{d_0}^2 u^2(d_0) + c_{\alpha}^2 u^2(\alpha) + c_{T_0}^2 u^2(T_0) + c_{T_m}^2 u^2(T_m) \quad (25)$$

$$c_{\Delta T}^2 u^2(\Delta T) = c_{\Delta T_0}^2 u^2(\Delta T_0) + c_{\Delta T_b}^2 u^2(\Delta T_b) + c_{\Delta T_c}^2 u^2(\Delta T_c) \quad (26)$$

where:

$$c_{P_0} = \frac{\partial \lambda(T_m)}{\partial P_0} = \frac{1}{N_1} \frac{Z_2}{N_2} \quad c_{\Delta T_0} = \frac{\partial \lambda(T_m)}{\partial \Delta T_0} = -\frac{Z_1}{N_1} \frac{Z_2}{N_2^2}$$

$$c_{P_x} = \frac{\partial \lambda(T_m)}{\partial P_x} = -\frac{1}{N_1} \frac{Z_2}{N_2} \quad c_{\Delta T_b} = \frac{\partial \lambda(T_m)}{\partial \Delta T_b} = \frac{Z_1}{N_1} \frac{Z_2}{N_2^2}$$

$$c_{\Sigma PV} = \frac{\partial \lambda(T_m)}{\partial \Sigma P_{Vi}} = -\frac{1}{N_1} \frac{Z_2}{N_2} \quad c_{\Delta T_c} = \frac{\partial \lambda(T_m)}{\partial \Delta T_c} = \frac{Z_1}{N_1} \frac{Z_2}{N_2^2}$$

$$c_{r_0} = \frac{\partial \lambda(T_m)}{\partial r_0} = -\frac{2Z_1}{N_1 r_0} \frac{Z_2}{N_2} \quad c_{d_0} = \frac{\partial \lambda(T_m)}{\partial d_0} = \frac{Z_1}{N_1} \frac{1}{N_2}$$

5.1.1. Geometry of Sample

Type A: The cylindrical sample should be plane-parallel and sharp-edged. The unavoidable deviations from plane parallelism are compensated for with silicone oil when coupling to the hot and cold plates takes place. The cross-sectional area of the sample, $A = \pi r^2$ (theoretical size: 7853.98 mm²), and its thickness d (theoretical size: 10 mm) are determined from a series of $N = 15$ observations. The uncertainties and variances according to Eq. (4) in relative terms are

$$u'(\bar{A}) = 2(0.05\%) = 0.1\%$$

and in absolute terms

$$u(\bar{A}) = 7.85 \times 10^{-6} \text{ m}$$

$$u^2(\bar{A}) = 6.2 \times 10^{-11} \text{ m}^2$$

and

$$u'(\bar{d}) = 0.05\%$$

$$u(\bar{d}) = 5 \times 10^{-6} \text{ m}$$

$$u^2(\bar{d}) = 2.5 \times 10^{-11} \text{ m}^2$$

respectively.

Type B: An estimate of $u(d)$ according to Eq. (6) and the statement “exact to 1/100 (mm)” furnishes:

$$u^2(d) = \frac{1}{12}(a_+ - a_-)^2 = \frac{1}{12}(10.01 \times 10^{-3} - 9.99 \times 10^{-3})^2 \text{ m}^2 = 3.33 \times 10^{-11} \text{ m}^2$$

$$u(d) = 5.8 \times 10^{-6} \text{ m}$$

At a working temperature $T_A = 20^\circ\text{C}$, the thermal expansion of the Pyrex sample need not be taken into consideration.

5.1.2. Temperature Differences

Type A: The observed mean values from 15 measurements of each of the ten individual temperatures, measured as thermoelectric voltage U_{Th} (cf., Fig. 1) and converted into temperatures T in accordance with the individual calibration tables, show a maximum standard deviation of 40 mK. The uncertainty $u(\Delta\bar{T})$ for the required temperature differences thus is:

$$u(\Delta\bar{T}) = \sqrt{(40 \times 10^{-3})^2 + (40 \times 10^{-3})^2} \text{ K} = 5.7 \times 10^{-2} \text{ K}$$

and the variance

$$u^2(\Delta\bar{T}) = 3.2 \times 10^{-3} \text{ K}^2.$$

Due to the great efforts which would have to be made, a description of the alternative determination of $u(\Delta T)$ by the *type B* procedure is not carried out.

5.1.3. Heat flow

Type A: The (gross) heat flow is determined from the electric input power $P = UI$ of the hot plate. For this purpose, the voltage drop U across the heater is directly measured and the current is determined indirectly from the voltage drop U_R across a calibrated four-pole standard resistor $R = 1 \Omega$. Thus $P = UU_R/R$ holds. Repeat observations show that the variance of the power is

$$u^2(\bar{P}) = 5.1 \times 10^{-8} \text{ W}^2.$$

Type B: For the DVM, the manufacturer specifies a resolution of $10 \mu\text{V}$ and maximum permissible errors (accuracy) of ± 10 ppm of the voltage reading $+4$ ppm for the ranges of measurement 3 and 30 V, respectively. These data have been verified by in-house calibration. For the measured value $U = 20 \text{ V}$, the resulting maximum permissible errors are $3.2 \times 10^{-4} \text{ V}$ and for the measured value $U_R = 0.5 \text{ V}$, according to the maximum permissible errors, $1.7 \times 10^{-5} \text{ V}$. With Eq. (6) the following two variances follow:

$$u^2(U) = 3.4 \times 10^{-8} \text{ V}^2$$

and

$$u^2(U_R) = 9.6 \times 10^{-11} \text{ V}^2.$$

The calibration certificate for the standard resistor $R = 1 \Omega$ confirms an uncertainty $u(\bar{R}) = 5 \times 10^{-6} \Omega$ so that the variance is given by

$$u^2(R) = 2.5 \times 10^{-11} \Omega^2.$$

Finally, the following relation is obtained for the variance of the quantity P using Eq. (1), the error propagation law:

$$u^2(P) = \left(\frac{U_R}{R}\right)^2 u^2(U) + \left(\frac{U}{R}\right)^2 u^2(U_R) + \left(\frac{UU_R}{R^2}\right)^2 u^2(R) = 4.7 \times 10^{-8} \text{ W}^2,$$

which still agrees quite well with the above-mentioned value.

5.1.4. Heat Flow Correction Factors

Type A: The values of the coefficients C_1 and C_2 from Eqs. (10) and (11) were determined by thermal mismatching (cf., Ref. 8); their individual uncertainties may be estimated at 5% at most. This relatively large value does not, however, exert such a substantial influence on the overall uncertainty budget; experience has shown that the correction factors P_{V1} and P_{V2} amount only to about 0.1% of P_0 . The relative uncertainty of P_{V3} is 20%, at most. Since $P_{V3}/P_0 \approx 0.1\%$ is valid, the influence on the uncertainty of the gross heat flow remains approximately 0.02%. Repeat observations furnish the following variances:

$$u^2(\bar{P}_{V1}) = 8.5 \times 10^{-7} \text{ W}^2.$$

$$u^2(\bar{P}_{V2}) = 8.5 \times 10^{-7} \text{ W}^2.$$

$$u^2(\bar{P}_{V3}) = 8.5 \times 10^{-7} \text{ W}^2.$$

This applies similarly to the quantity P_X . Here, the uncertainty of 0.08% is obtained from the series of measurements. The resulting variance is

$$u^2(\bar{P}_X) = 1.5 \times 10^{-7} \text{ W}^2.$$

The stray heat flow P_{V4} from the edge heat loss error (gap) for the guard plate can be neglected because the working temperature is 20°C. The stray heat flow P_{V5} from the heat loss error at the sample's lateral surface may also be neglected, as the thermal conductivity of the Pyrex sample under test is still high compared with the thermal conductivity of the protective ring (Fig. 1: element (F)).

Type B: A determination of the variances of the stray heat flows by the *type B* procedure is most complicated as the mathematical relations are indeterminate.

5.2. Specimen-Specific Corrections

The temperature jump at the front faces of the specimen in most cases cannot be adequately described mathematically. The influence must be estimated for each individual case. For the measurement on Pyrex glass, this effect may certainly be neglected. The second sample-specific effect mentioned above, the radiative transport in the sample, need not be corrected either. Infrared absorption spectra on Pyrex measured at PTB do not show significant transpance in the working temperature range of the guarded hot plate.

5.3. Covariances

To determine the electric input power, $P = UU_R/R$, the voltages U and U_R are measured using the same voltmeter. Thus, the associated uncertainty contributions are, strictly speaking, correlated. This effect leads to an increase in the uncertainty because the product of both voltages appears. However, compared with the uncertainty in determining the rate of heat flow (cf., Section 5.1.3) the contribution due to correlation is negligible.

5.4. Uncertainty Budget

Table III contains all data important for the uncertainty analysis such as input quantities, their estimated values as well as the associated sensitivity coefficients and the variances determined.

The absolute standard uncertainty to be assigned to the measurement result on Pyrex at 20°C (cf. Section 4.2.3.) reads:

$$u(\lambda) = \sqrt{1.21 \times 10^{-4} \text{ W}^2 \cdot \text{m}^{-2} \cdot \text{K}^{-2}} = 0.011 \text{ W} \cdot \text{m}^{-1} \cdot \text{K}^{-1}$$

Just as here, a normal distribution can generally be assigned to the measurand. The result given then is valid for a coverage probability of 68.3%. With this probability the measured value lies in the confidence interval $\pm u(\lambda)$. According to the resolution adopted by the EA (European Cooperation for Accreditation), a so-called expanded uncertainty of measurement $U(\lambda) = 2u(\lambda)$ should be stated. The coverage probability for the coverage factor 2 then is 95%. The uncertainty of measurement thus is:

$$U(\lambda) = 2 \cdot (0.011) \text{ W} \cdot \text{m}^{-1} \cdot \text{K}^{-1} = 0.022 \text{ W} \cdot \text{m}^{-1} \cdot \text{K}^{-1}$$

In relative terms, this reads $U'(\lambda) = (0.022/1.13) \cdot 100 = 1.9\%$.

According to the GUM, the numerical value of the uncertainty is to be stated with two significant digits at most. The complete measurement result for this example is $\lambda = (1.13 \pm 0.02) \text{ W} \cdot \text{m}^{-1} \cdot \text{K}^{-1}$.

It is immediately apparent from Table III that the effect of the uncertainty in the power P_0 measurement is negligible relative to the influence of the other quantities. The uncertainties in temperature measurements are the greatest.

Figure 2 presents the expanded uncertainty over the whole measurement range of the instrument analyzed. From its upper end at 6 to $0.1 \text{ W} \cdot \text{m}^{-1} \cdot \text{K}^{-1}$, the uncertainty is almost constant. At the lower end of the range of $0.02 \text{ W} \cdot \text{m}^{-1} \cdot \text{K}^{-1}$, the uncertainty increases to 2.9%.

To check the ability of the model presented, the uncertainty obtained was experimentally verified against the CRM 039 standard mentioned

Table III. Uncertainty Budget

Quantity X_i	Estimate x_i	Probability distrib.	Sensitivity coeff. $c_i = (\partial f(x)/\partial x_i)$	Stand. unc. $u(x_i)$	$u_i(y)$
P_0	8.9 W	normal	$1.27 \times 10^{-1} \text{ m}^{-1} \cdot \text{K}^{-1}$	$2.3 \times 10^{-4} \text{ W}$	$2.9 \times 10^{-5} \text{ W} \cdot \text{m}^{-1} \cdot \text{K}^{-1}$
P_x	0 W	normal	$1.27 \times 10^{-1} \text{ m}^{-1} \cdot \text{K}^{-1}$	$3.9 \times 10^{-4} \text{ W}$	$5.0 \times 10^{-5} \text{ W} \cdot \text{m}^{-1} \cdot \text{K}^{-1}$
P_{V1}	0 W	normal	$-1.27 \times 10^{-1} \text{ m}^{-1} \cdot \text{K}^{-1}$	$9.2 \times 10^{-4} \text{ W}$	$-1.2 \times 10^{-4} \text{ W} \cdot \text{m}^{-1} \cdot \text{K}^{-1}$
P_{V2}	0 W	normal	$-1.27 \times 10^{-1} \text{ m}^{-1} \cdot \text{K}^{-1}$	$9.2 \times 10^{-4} \text{ W}$	$-1.2 \times 10^{-4} \text{ W} \cdot \text{m}^{-1} \cdot \text{K}^{-1}$
P_{V3}	0 W	normal	$-1.27 \times 10^{-1} \text{ m}^{-1} \cdot \text{K}^{-1}$	$9.2 \times 10^{-4} \text{ W}$	$-1.2 \times 10^{-4} \text{ W} \cdot \text{m}^{-1} \cdot \text{K}^{-1}$
A_0	$7853.98 \times 10^{-6} \text{ m}^2$	rectangular	$-1.44 \times 10^2 \text{ W} \cdot \text{m}^{-3} \cdot \text{K}^{-1}$	$7.9 \times 10^{-6} \text{ m}^2$	$-1.1 \times 10^{-3} \text{ W} \cdot \text{m}^{-1} \cdot \text{K}^{-1}$
d_0	$10 \times 10^{-3} \text{ m}$	rectangular	$1.13 \times 10^2 \text{ W} \cdot \text{m}^{-2} \cdot \text{K}^{-1}$	$5.0 \times 10^{-6} \text{ m}$	$5.8 \times 10^{-4} \text{ W} \cdot \text{m}^{-1} \cdot \text{K}^{-1}$
ΔT_0	10 K	normal	$1.13 \times 10^{-1} \text{ W} \cdot \text{m}^{-1} \cdot \text{K}^{-2}$	$5.7 \times 10^{-2} \text{ K}$	$6.4 \times 10^{-3} \text{ W} \cdot \text{m}^{-1} \cdot \text{K}^{-1}$
ΔT_b	0 K	normal	$1.13 \times 10^{-1} \text{ W} \cdot \text{m}^{-1} \cdot \text{K}^{-2}$	$5.7 \times 10^{-2} \text{ K}$	$6.4 \times 10^{-3} \text{ W} \cdot \text{m}^{-1} \cdot \text{K}^{-1}$
ΔT_c	0 K	normal	$1.13 \times 10^{-1} \text{ W} \cdot \text{m}^{-1} \cdot \text{K}^{-2}$	$5.7 \times 10^{-2} \text{ K}$	$6.4 \times 10^{-3} \text{ W} \cdot \text{m}^{-1} \cdot \text{K}^{-1}$
λ	$1.13 \text{ W} \cdot \text{m}^{-1} \cdot \text{K}^{-1}$				$0.011 \text{ W} \cdot \text{m}^{-1} \cdot \text{K}^{-1}$

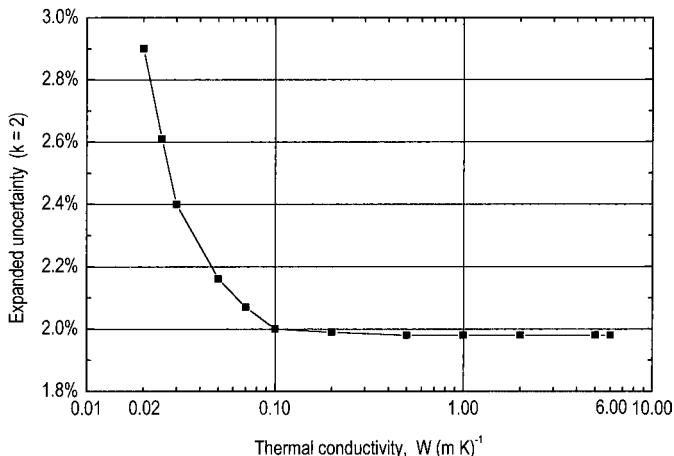


Fig. 2. Uncertainty analysis result over the whole measurement range.

above. The maximum deviation from the reference values (having itself an uncertainty of 1.2%) was found to be at most 0.4%.

6. CONCLUSION

According to the Vocabulary of Basic and General Terms in Metrology [15], the complete statement of a measurement result contains not only the measured value but also information about its uncertainty. For reasons of uniformity and comparability, this information which characterizes the quality of the measurement should be determined in accordance with the ISO Guide to the Expression of Uncertainty in Measurement [6] and stated as an expanded standard uncertainty of measurement.

To estimate the uncertainty, two different methods are available. One of these is the purely statistical type A method which should be given preference over the type B method, if possible. For a computer-controlled guarded hot plate as the one discussed above, the type A method can be integrated without any difficulties into the measurement and evaluation program so that at the end the computer outputs a “true measurement result.”

REFERENCES

1. K. D. Maglic (ed.), A. Cezairliyan, and V. E. Peletsky, in *Compendium of Thermophysical Property Measurement Methods* (Plenum Press, New York and London, 1984), Vol. 1.

2. DIN 52612, *Bestimmung der Wärmeleitfähigkeit mit dem Plattengerät* (Beuth Verlag GmbH, Berlin, 1979).
3. ASTM C 201-86, The American Society for Testing and Materials 1986.
4. ISO 8302, *Thermal Insulation, Guarded hot plate apparatus* (Beuth Verlag GmbH, Berlin, 1996).
5. VDI 2055, *Wärme- und Kälteschutz für betriebs- und haustechnische Anlagen* (Beuth Verlag, Berlin, 1994).
6. ISO, *Guide to the Expression of Uncertainty in Measurement* (1993).
7. W. Hemminger and R. Jugel, *Int. J. Thermophys.* **6**:483 (1985).
8. H. Poltz and R. Jugel, *Int. J. Heat Mass Transfer* **25**:1093 (1982).
9. W. Woodside and A. G. Wilson, Symposium on Thermal Conductivity Measurements and Applications of Thermal Insulations, ASTM STP217, ASTTA, Am. Soc. Testing Mats. 32 (1956).
10. W. Woodside, Symposium on Thermal Conductivity Measurements and Applications of Thermal Insulations, ASTM STP217, ASTTA, Am. Soc. Testing Mats. 49 (1956).
11. W. Fritz and K.-H. Bode, *Chem. Ing. Tech.* **37**:1118 (1965).
12. K.-H. Bode, *Int. J. Heat Mass Transfer* **23**:961 (1980).
13. U. Wolfseher, Diss. (Univ. Gesamthochschule, Essen, 1978).
14. F. Adunka, *Mefßunsicherheiten* (Vulkan Verlag, Essen, 1998).
15. DIN, ed., *Internationales Wörterbuch der Metrologie*, 2. Auflage (Beuth Verlag GmbH, Berlin, 1994).